24th INTERNATIONAL CONGRESS ON SOUND AND VIBRATION
23–27 July 2017, London

MULTIPLE VIBRATION BAND GAPS IN LOCALLY RESONANT BEAM CARRYING SINGLE PERIODIC ARRAY OF CANTILEVER BEAM TYPE RESONATORS

Xuezhi Zhu, Zhaobo Chen and Yinghou Jiao

Harbin Institute of Technology, School of Mechatronics Engineering, Harbin, China
email: zxz0001zxz@126.com

In this paper, the property of multiple vibration band gaps in locally resonant beam carrying beam type resonators is investigated. Small sized beams are attached to one host beam to combine into a locally resonant beam containing cantilever beam type resonators. Numerical and experimental analyses show that this type of locally resonant beam can generate a plurality of locally resonant band gaps. Equivalent multiple resonators model of the cantilever beam type resonator is established according to modal superposition theory. Each mode of the cantilever beam type resonator is equivalent to a single degree of freedom spring-mass oscillator system while effective modal mass and effective modal stiffness of each mode are as the lumped mass and stiffness of the oscillator system respectively. Equivalent multiple resonators model is verified by dynamic stiffness and dispersion relation results. The multi-band gaps induced by cantilever beam type resonator are verified theoretically and experimentally. The band structure of the locally resonant beam containing equivalent multiple resonators model is consistent with the one of the locally resonant beam containing cantilever beam type resonators model indicating the high accuracy of equivalent method. Experimental work also verified that locally resonant band gap could be broadened effectively after laying damping layer on the cantilever beam type resonator while greater damping can be achieved at higher order modes.
Keywords: locally resonant beam, beam type resonator, multi-band gaps, equivalent multiple resonators model, effective modal mass

1. Introduction

The phononic crystals (PCs) had been proposed 30 years ago, elastic wave band gap is one of the most important properties [1,2]. According to the locally resonant band gap mechanism [3], the small sized PCs structure can also generate low frequency band gap. So locally resonant PCs (LRPCs) has a broad application prospects of vibration reduction.

Researchers usually embed metal balls coated with rubber layers into the base material or attach resonators onto the beams and plates to form the PCs [4,5]. These LRPCs have less band gaps because resonators in these models have less resonant modes. However, the locally resonant band gaps are dependent on these modes [6]. Researchers usually wish to obtain broad band or multiple band vibration reduction using multiple vibration absorbers such as distributed dynamic vibration absorbers [7-10].

Beam type vibration absorbers have broadband vibration suppression property because the beam has rich modes. M. Cavacece et al. [11] applied the beam type dynamic vibration absorber to SDOF vibration system, then optimized the beam parameters. Brenan et al. [12] proposed equivalent mass of the cantilever beam type vibration absorber which only involves the first mode. Xiao Yong et al. took the cantilever beam as SDOF resonator in the LRPCs structure and determined the equivalent mass of the cantilever beam type resonator(CB resonator) [13].

In the previous study, only the first mode of the CB resonator is focused. However, the high order modes can also result in obvious band gaps. Slight changes in mass of the resonators may lead to obvious alternating in bandwidth, one should determine the mass of the CB resonator in order to tune the band gap. In this paper, equivalent multiple resonators (M-SDOF resonator) model of CB resonator involving multiple modes is proposed and the equivalent mass which has great influence on bandwidth is identified. Multi-band gap induced by the CB resonator of the LR beam is clarified by theoretical and experimental analysis.

2. Equivalent model of CB resonator

2.1 Equivalent M-SDOF model of the CB resonator

Cantilever beams are periodically attached to a main beam to form a simple Euler LR beam. The cross section of the LR beam is rectangular, width and height are set to b, h, lattice constant is a, as shown in Fig. 1. Take the central axis of the no deformed LR beam as the x-axis. There is only flexural vibration in the LR beam and CB resonator in y direction.

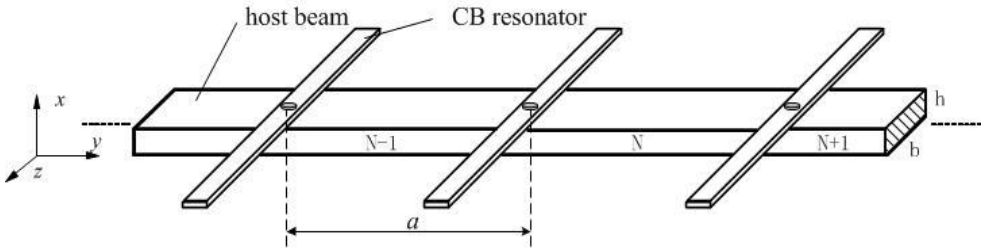

Figure 1: LR beam containing CB resonator.

Figure 2. is a schematic of CB resonator and equivalent spring-mass oscillator model. CB resonator is usually used in pairs as shown in the Fig. 2(a), the length of the CB resonator is set to$l$, the cross section is rectangular with the width and height are set to b_{r} , h_{r} respectively, the length of the cantilevered portion is l_{r} while the length of the connecting portion in the root of the CB resonator is $l_{\mathrm{s}} = 2(l - l_{\mathrm{r}})$.

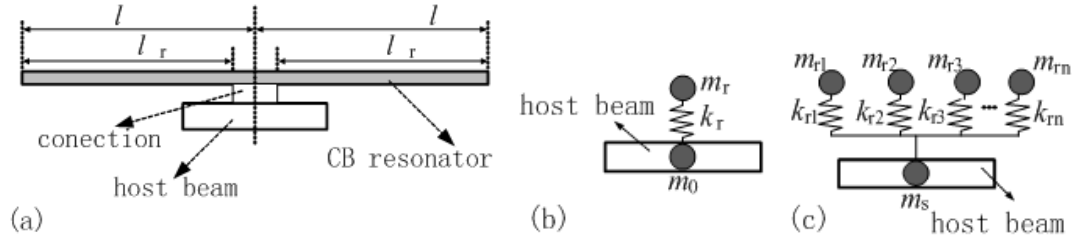

Figure 2: (a) Schematic of CB resonator connected with host structure; (b) Equivalent single resonator model; (c) Equivalent M-SDOF resonator model.

Currently, the CB resonator is equivalent to a SDOF resonator as shown in the Fig. 2(b) with the equivalent lump mass m_r=0.605$\rho_{\mathrm{r}}\mathrm{A}_{\mathrm{r}}$, where $\rho_{\mathrm{r}}, \mathrm{A}_{\mathrm{r}}$ is density and cross-sectional area of the CB resonator respectively, the rest mass of the cantilevered portion constitute m_0 with m_s, where m_s=$\rho_{\mathrm{r}}\mathrm{A}_{\mathrm{r}}l_{\mathrm{s}}$.

Considering multiple modes, CB resonator should be equivalent to M-SDOF resonator model shown in Fig. 2 (c). The key point of the equivalent process is to determine the equivalent mass $m_{\mathrm{r}i}$ and equivalent stiffness $k_{\mathrm{r}i}$ of each mode. Effective mode mass of the CB resonator is appropriate to be as the lump masses of the equivalent M-SDOF resonator. Effective mode mass is a coefficient which is usually used in vibration response calculation by modal superposition method [14].

For a MDOF vibration system, the vibration equation can be expressed as

$$\boldsymbol{M\ddot{X} + C\dot{X} + KX = F} \tag{1}$$

Where $\boldsymbol{M}$, $\boldsymbol{C}$ and $\boldsymbol{K}$ is mass matrix, damping matrix and stiffness matrix respectively. $\boldsymbol{X}$, $\boldsymbol{F}$ is displacement vector and the force vector respectively.

Let $\boldsymbol{\varphi}$ be the eigenvector matrix, the generalized mass matrix for mode i of the system is given by

$$\boldsymbol{M_i} = \boldsymbol{\varphi}_i^{\mathrm{T}} \boldsymbol{M} \boldsymbol{\varphi}_i \tag{2}$$

When the external force at the root of the cantilever beam is along the transverse direction i.e. y direction, define parameter $\boldsymbol{L_i}$ for the mode i as

$$\boldsymbol{L_i} = \boldsymbol{\varphi}_i^{\mathrm{T}} \boldsymbol{M} \boldsymbol{I} \tag{3}$$

Where $\boldsymbol{I}$ is a unit vector. The modal participation factor matrix $\boldsymbol{\gamma_i}$for mode i is

$$\boldsymbol{\gamma_i} = \frac{\boldsymbol{L_i}}{\boldsymbol{M_i}} \tag{4}$$

The effective modal mass for mode i is

$$m_{e,i} = \boldsymbol{M_i} \boldsymbol{\gamma_i^2} \tag{5}$$

Effective modal mass has mass dimension and the sum of all mode's effective modal mass is equal to the total mass of the system in each direction.

$$\sum_{i=1}^{\mathrm{n}} m_{eix} = \sum_{i=1}^{\mathrm{n}} m_i \tag{6}$$

Where n represents an n DOF system, x represents along x direction, $\sum_{i=1}^{\mathrm{n}} m_i$ represents the total mass of the system.

The definition of effective modal mass for mode i of Bernoulli - Euler beam is [15]

$$m_{\mathrm{e},i} = \frac{\left[\int_0^{\mathrm{L}} \rho(x) \mathrm{Y}_i(x) \mathrm{d}x\right]^2}{\int_0^{\mathrm{L}} \rho(x) [\mathrm{Y}_i(x)]^2 \mathrm{d}x} \tag{7}$$

where $\rho(x)$ is mass per length, $\mathrm{Y}_i(x)$ is mass-normalized eigenvector for mode i.

For CB resonator, the equivalent mass for mode i of the equivalent M-SDOF resonator is exactly the effective modal mass

$$m_{\mathrm{r}i} = m_{\mathrm{e},i} \tag{8}$$

It's easy to get natural frequency $\omega_{\mathrm{r}i}$ of the CB resonator, and equivalent stiffness of the equivalent M-SDOF resonator should be

$$k_{\mathrm{r}i} = m_{\mathrm{r}i} {\omega_{\mathrm{r}i}}^2 \tag{9}$$

Only considering the first four modes of the CB resonator, the equivalent mass of each mode is shown in Table 1.

Table 1: Equivalent mass

Mode	Natural frequency $\boldsymbol{\omega_{ri}}$	Equivalent mass $\boldsymbol{m_{ri}}$
1	$1.875104^2 \sqrt{\frac{E_r I_r}{\rho_{\mathrm{r}} A_{\mathrm{r}} l_{\mathrm{r}}^4}}$	$0.6131 \rho_{\mathrm{r}} A_{\mathrm{r}} l_{\mathrm{r}}$
2	$4.694091^2 \sqrt{\frac{E_r I_r}{\rho_{\mathrm{r}} A_{\mathrm{r}} l_{\mathrm{r}}^4}}$	$0.1883 \rho_{\mathrm{r}} A_{\mathrm{r}} l_{\mathrm{r}}$
3	$7.854757^2 \sqrt{\frac{E_r I_r}{\rho_{\mathrm{r}} A_{\mathrm{r}} l_{\mathrm{r}}^4}}$	$0.06474 \rho_{\mathrm{r}} A_{\mathrm{r}} l_{\mathrm{r}}$
4	$10.995541^2 \sqrt{\frac{E_r I_r}{\rho_{\mathrm{r}} A_{\mathrm{r}} l_{\mathrm{r}}^4}}$	$0.03306 \rho_{\mathrm{r}} A_{\mathrm{r}} l_{\mathrm{r}}$

2.2 Validation of the equivalent M-SDOF model

Driving-point dynamic stiffness is used to evaluate the correctness of equivalent M-SDOF model.

Neglecting the mass of the connecting bolts and gaskets, driving-point dynamic stiffness of the connecting portion of the CB resonator is

$$\mathrm{D_s} = -\omega^2 m_s \tag{10}$$

The driving-point dynamic stiffness of the l_r portion is[13]

$$\mathrm{D_c} = \frac{-E_\mathrm{r} I_\mathrm{r} (\beta_\mathrm{r} l_\mathrm{r})^3}{l_\mathrm{r}^3} \frac{\cos(\beta_\mathrm{r} l_\mathrm{r})\sinh(\beta_\mathrm{r} l_\mathrm{r}) + \sin(\beta_\mathrm{r} l_\mathrm{r})\cosh(\beta_\mathrm{r} l_\mathrm{r})}{1 + \cos(\beta_\mathrm{r} l_\mathrm{r})\cosh(\beta_\mathrm{r} l_\mathrm{r})}, \beta_\mathrm{r} = \left(\frac{\rho_r A_r \omega^2}{-E_\mathrm{r} I_\mathrm{r}}\right)^{1/4} \tag{11}$$

Where β_r is flexural wave number, $E_\mathrm{r}, I_\mathrm{r}$ is Young's modulus and second moment of cross-section of the CB resonator.

Total driving-point dynamic stiffness of the CB resonator shown in Fig. 2(a) is

$$\mathrm{D_r} = \mathrm{D_s} + 2\mathrm{D_c} \tag{12}$$

Driving-point dynamic stiffness for mode *i* of the equivalent M-SDOF resonator is

$$\mathrm{D}_{\mathrm{r}i} = \frac{-\omega^2 m_{\mathrm{r}i}}{1 - \omega^2/\omega_{\mathrm{r}i}^2} \tag{13}$$

Concerning first n mode of the CB resonator, the total driving-point dynamic stiffness of the equivalent M-SDOF resonator is

$$\mathrm{D_{e,n}} = \mathrm{D_s} + \sum_{i=1}^{\mathrm{n}} \mathrm{D}_{\mathrm{r}i} \tag{14}$$

The geometry and material parameters of CB resonator is shown in Table 2.

Table 2: Parameters of CB resonator

l	116mm	h_r	2mm
l_r	101mm	ρ_r	8500kg/m^3
b_r	30mm	E_r	100Gpa

The driving-point dynamic stiffness of CB resonator and equivalent M-SDOF resonator is compared in Fig. 3.

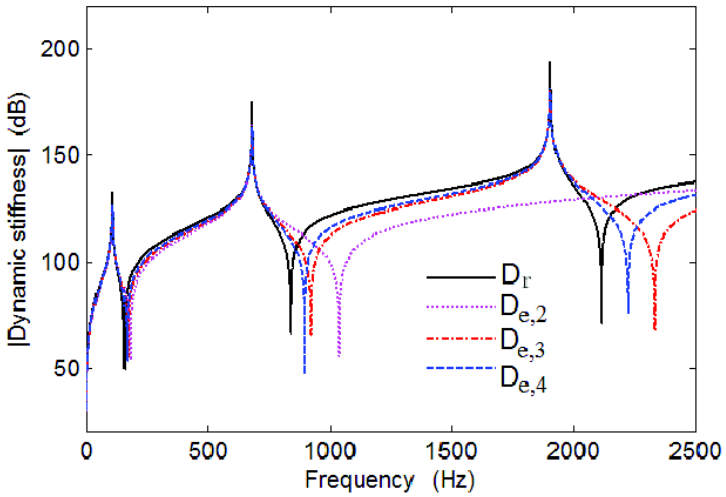

Figure 3: driving-point dynamic stiffness of CB resonator.

CB resonator has 3 vibration modes in 0-2500Hz frequency band while its dynamic stiffness has a peak value at each modal frequency. The dynamic stiffness of the equivalent M-SDOF resonator has the same peak frequency with the one of CB resonator. Dynamic stiffness value of the equivalent M-SDOF resonator has deviation with the exact dynamic stiffness of CB resonator due to the modal truncation when a limited number of modes of the CB resonator are involved in

equivalent M-SDOF resonator. The dynamic stiffness value of the equivalent M-SDOF resonator will goes much closer with the exact dynamic stiffness value when more modes of the CB resonator are introduced.

3. Band gaps of the LR beam

In this paper, the disperse relation equation of the LR beam carrying periodic array of spring-mass resonators derived by spectral element method is used directly to get the band structure [13].

$$cos^2(qa) + \alpha_1 \cos(qa) + \alpha_2 = 0 \tag{15}$$

Where

$$\alpha_1 = -[-\cos(k_b a) + \cosh(k_b a)] - \frac{\mathrm{D_r}}{4EIk_b{}^3}[\sin(k_b a) + \sinh(k_b a)] \tag{16}$$

$$\alpha_2 = \cos(k_b a)\cosh(k_b a) + \frac{\mathrm{D_r}}{4EIk_b{}^3}[\sin(k_b a)\cosh(k_b a) - \cos(k_b a)\sinh(k_b a)] \tag{17}$$

$$k_b = (\frac{\rho A\omega^2}{EI})^{1/4} \tag{18}$$

In the above, k_b denotes the flexural wave number of the host beam. ρ, E, A and I is material density, Young's modulus, cross-sectional area and second moment of cross-section of the host beam.

Set the material of the host beam as steel, the Young's modulus is $E = 220\mathrm{GPa}$, material density is ρ =7850kg/m^3. Set geometric parameters as b=40mm, h=5mm, a=100mm. The band structure of the LR beam is demonstrated in Fig. 4.

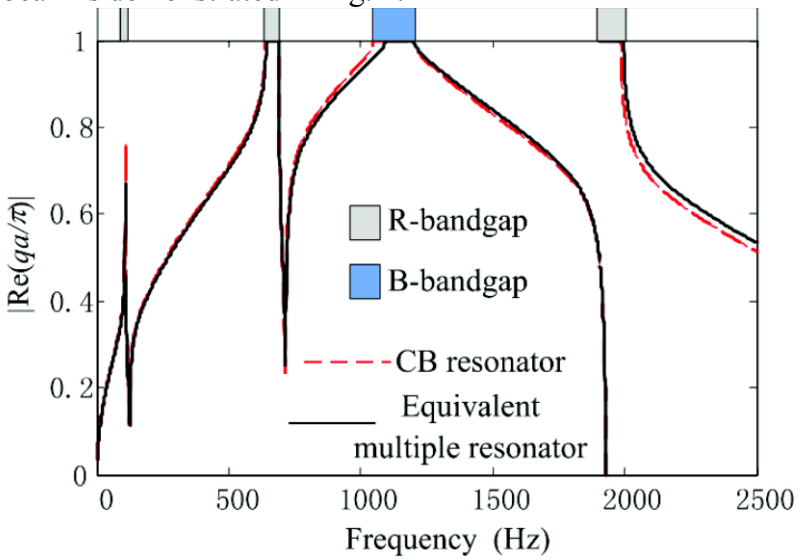

Figure 4: band structure of LR beam.

The curves shown in the Fig. 4 are amplitude of the real part of Bloch wave vector qa/π. The frequency ranges of $|\mathrm{Re}(qa/\pi)| < 1$are wave propagation bands while the other ranges are band gaps. The colour bars represent 4 band gaps in 0-2500Hz. The solid line and broken line represent the band structure of the LR beam carrying CB resonator model and equivalent M-SDOF resonator model respectively. This two resonator models produce two similar band structures showing the accuracy of the equivalent M-SDOF resonator model. Four band gaps in Fig. 4 are divided into two types while the light blue bar represents the first Bragg gap (B-bandgap) whose cutoff frequency is the first Bragg frequency

$$f_{\mathrm{B},1} = \frac{1}{2\pi}(\frac{\pi}{a})^2\sqrt{\frac{EI}{\rho \mathrm{A}}} = 1200\mathrm{Hz} \tag{19}$$

LR beam carrying two type resonator model has the same Bragg frequency because the Bragg frequency is independent of the resonator. The grey bar represents locally resonant band gap (R-bandgap) whose position and width have great relationship with the resonant frequency and mass of the resonator. The position and width of the R-bandgap induced by two type resonator model are consistent showing the accuracy of the equivalent multiple resonator model.

4. Vibration transmission of the LR beam

LR beam is infinite periodic structure in band structure theory analysis while only limit sized periodic structure can be used in practical engineering application. Elastic wave band gap of the infinite periodic PCs is usually verified by vibration transmission of the corresponding finite periodic structure. Finite element method (FEM) method is very convenient in analysing vibration transmission characteristics of the finite LR beam. Take FEM software MSC.PATRAN/NASTRAN as the analysis tool, FE model of the LR beam containing 10 cells is shown in Fig. 5, size and material parameters of the FE model are coincident with the parameters in theory analysis above.

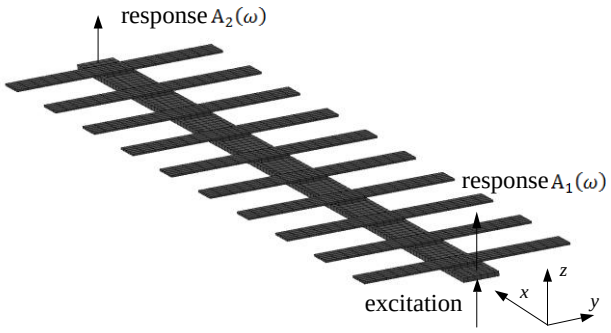

Figure 5: FE model of the LR beam.

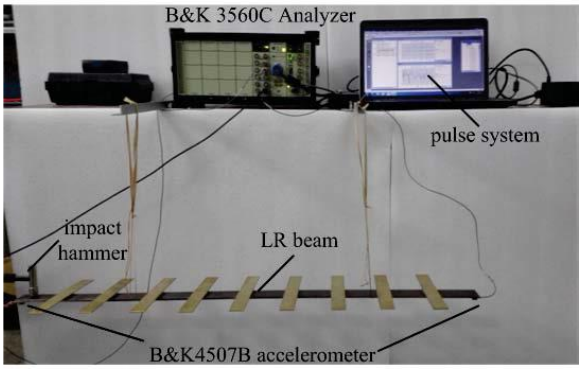

Figure 6: experimental test setting.

The sinusoidal excitation of amplitude of 1N with bandwidth from 0 to 2500Hz is applied to the left end and pike up vibration acceleration response $A_1(\omega)$, $A_2(\omega)$ at both end of the finite LR beam. Vibration transmission FRF can be obtained as

$$T = \left|\frac{A_2(\omega)}{A_1(\omega)}\right| \tag{20}$$

In order to verify the results of the theoretical and numerical calculations, an experimental sample having same material and geometric parameters with the FE model is fabricated to test vibration transmission FRF. The sample is suspended with elastic ropes to set a free boundary condition. Strike one end of the LR beam sample using B&K2301 impact hammer along *z* direction to give an impact excitation. Hard hammer head is used to get a broadband force excitation covering 0-2500Hz.The transverse vibration response at the both end are picked up by B&K4507B accelerometers as shown in Fig. 6.

Figure 7 shows the vibration transmission FRF of the LR beam sample which is measured and post analysed by B&K pulse system. Vibration transmission test result (displayed as solid line) shows that CB resonator produce 5 vibration transmission band gaps which are represented as grey bars A, B, C, D and E. FEM calculation result is also plotted as broken line in Fig. 7, the calculated vibration transmission band gaps in position A, B and D are consistent with the R-bandgap in Fig. 4. Band gaps C and E do not appear in the wave band structure because CB resonator only has bending vibration mode in wave band structure theoretical calculations while other type of vibration mode exist in vibration transmission analysis.

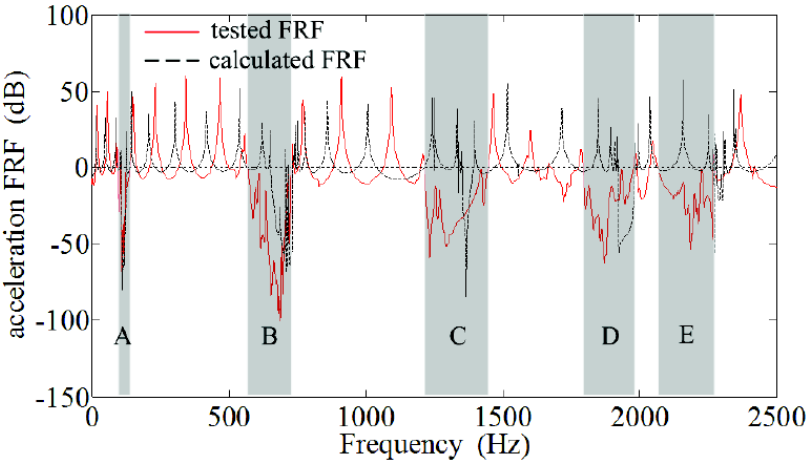

Figure 7: Vibration transmission FRF of LR beam.

Damping effect is also studied through Experimental test. Relevant research has suggested that damping added in the resonator could effectively broaden the width of the LR band gap. Although the damping effect is easy to clarify through theory analysis, there is no experimental verification until now, and great damping improvement is not easy in reality. The benefit of taking cantilever beam as the resonator of the LR beam is the ability of adding more damping into the resonator system through laying damping layer on the surface of the CB resonator. According to energy dissipation mechanism of damping material, greater damping could be obtained when more deformation of the damping material occurs. CB resonator could bring great damping effect within multi frequency band because of its rich modal deformation.

The experimental vibration transmission FRF is shown in Fig. 8 and the picture of CB resonator with damping layer on the surface is inserted in the bottom right corner. The solid and broken lines represent the vibration transmission FRF of the LR beam with and without damping layer on CB resonator. After laying damping layer, the vibration transmission band gaps A, B, C, D and E are broadened with effect of 3Hz, 35 Hz, 100 Hz, 127 Hz and 101 Hz respectively. More vibration modes of CB resonator should be concerned because greater damping could be introduced at high order modes.

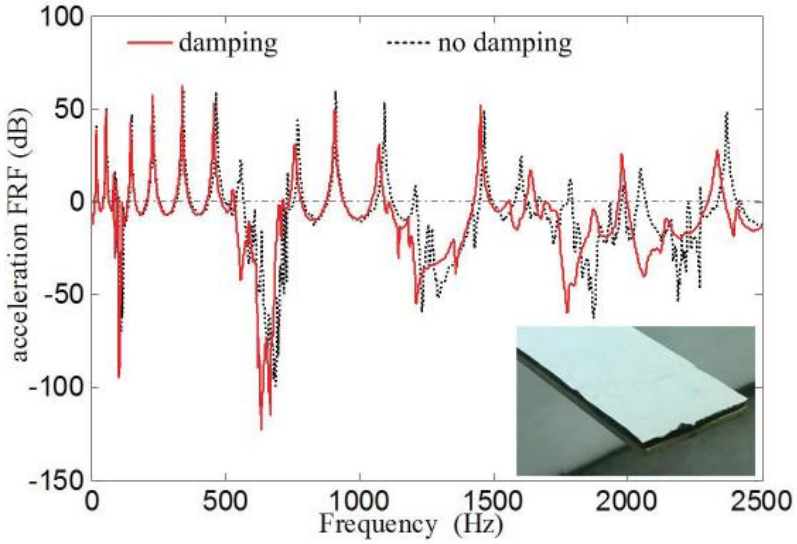

Figure 8: experimental result of damping effect.

5. Conclusion

In this paper, the property of multiple vibration band gaps in LR beam carrying single periodic of CB resonators are investigated. Equivalent M-SDOF model of the CB resonator is established. Each

mode of the CB resonator is one SDOF resonator of the equivalent M-SDOF model while the corresponding effective mode mass is correctly the equivalent lump mass of the SDOF resonator. Dispersion relation of the LR beam is calculated through spectrum element method. The equivalent M-SDOF model could produce same band structure with the practical CB resonator model, validating the high accuracy of the Equivalent M-SDOF model. The equivalent M-SDOF model of CB resonator could offer accurate parameters to improve broadband vibration gap design. The multiple band gaps induced by CB resonator are verified through experimental vibration transmission test. Experimental test also show that band gaps could be broadened effectively laying damping layer on the CB resonator. CB resonator has great advantage in broadening vibration transmission band gap.

REFERENCES

1 A. G. Every, a field that has come of age, *Ultrasonics* **54** (1), 1 (2014).

2 J. Mei, G. Ma, M. Yang, Z. Yang, W. Wen and P. Sheng, Dark acoustic metamaterials as super absorbers for low-frequency sound, *Nature communications* **3**, 756 (2012).

3 Z. Liu, X. Zhang, Y. Mao, Y. Y. Zhu, Z. Yang, C. T. Chan, and P. Sheng, Dynamic Mass Density and Acoustic Metamaterials, *Science* **289**, 1734(2000).

4 Z. Liu, C. T. Chan and P. Sheng, Analytic model of phononic crystals with local resonances, *Physical Review B* **71** (1) (2005).

5 Y. Xiao, J. Wen, D. Yu and X. Wen, Flexural wave propagation in beams with periodically attached vibration absorbers: Band-gap behavior and band formation mechanisms, *Journal of Sound and Vibration* **332** (4), 867-893 (2013).

6 K. Yu, T. Chen and X. Wang, Large band gaps in two-dimensional phononic crystals with neck structures, *Journal of Applied Physics* **113** (13), 134901 (2013).

7 A. O. Krushynska, V. G. Kouznetsova and M. G. D. Geers, Towards optimal design of locally resonant acoustic metamaterials, *Journal of the Mechanics and Physics of Solids* **71**, 179-196 (2014).

8 S. J. Jang and Y. J. Choi, Geometrical design method of multi-degree-of-freedom dynamic vibration absorbers, *Journal of Sound and Vibration* **303** (1-2), 343-356 (2007).

9 C. Yang, D. Li and L. Cheng, Dynamic vibration absorbers for vibration control within a frequency band, *Journal of Sound and Vibration* **330** (8), 1582-1598 (2011).

10 D. J. Thompson, A continuous damped vibration absorber to reduce broad-band wave propagation in beams, *Journal of Sound and Vibration* **311** (3-5), 824-842 (2008).

11 M. Cavacece,L. Vita, Optimal cantilever dynamic vibration absorbers by Timoshenko Beam Theory,*Shock and Vibration* **11**,199-207(2002).

12 H. M. El-Khatib, B. R. Mace and M. J. Brennan, Suppression of bending waves in a beam using a tuned vibration absorber, *Journal of Sound and Vibration* **288** (4-5), 1157-1175 (2005).

13 Y. Xiao, J. Wen, G. Wang and X. Wen, Theoretical and Experimental Study of Locally Resonant and Bragg Band Gaps in Flexural Beams Carrying Periodic Arrays of Beam-Like Resonators, *Journal of Vibration and Acoustics* **135** (4), 041006 (2013).

14 Patrick Paultre, *Dynamics of Structures*, Wiley, New York, (1986).

15 T. Irvine, effective modal mass & modal participation factors, *Revision H, Vibrationdata,* (2013).